Journal of Alloys and Compounds 631 (2015) 99–104

Contents lists available at ScienceDirect

Journal of Alloys and Compounds

journal homepage: www.elsevier.com/locate/jalcom

A simple method for determining the lattice parameter and chemical composition in ternary bcc-Fe rich nanocrystals

Javier A. Moya [a,*], Soledad Gamarra Caramella [a], Leonardo J. Marta [a], Carlos Berejnoi [b]

[a] Grupo Interdisciplinario en Materiales-IESIING, Universidad Católica de Salta, INTECIN UBA-CONICET, Salta, Argentina
[b] Universidad Nacional de Salta, Facultad de Ingeniería, Salta, Argentina

ARTICLE INFO

Article history:
Received 19 December 2014
Accepted 7 January 2015
Available online 23 January 2015

Keywords:
Nanostructured materials
Metals and alloys
Crystal structure
Phase diagrams
X-ray diffraction
Mössbauer spectroscopy

ABSTRACT

Charts containing lattice parameters of $Fe_{1-x}(M,N)_x$ ternary systems with M and N = Si, Al, Ge or Co, and $0 \leqslant x \leqslant \sim 0.3$, were developed by implementing a linear relationship between the respective binary alloys with the same solute content of the ternary one. Charts were validated with experimental data obtained from literature. For the Fe–Co–Si system, the linear relationship does not fit the experimental data. For the other systems (except the Fe–Co–Ge one where no experimental data was found), the lineal relationship constitute a very good approximation. Using these charts and the lattice parameter data obtained from X-ray diffraction technique combining with the solute content data obtained from Mössbauer spectroscopy technique it is possible to determine the chemical composition of nanograins in soft magnetic nanocomposite materials and some examples are provided.

1. Introduction

Nanocrystalline soft magnetic materials are composed of typically 10–25 nm diameter grains immersed in an amorphous matrix. Besides the grain diameter, soft magnetic properties strongly depend on the magnetocrystalline anisotropy and the magnetostriction constant of the crystalline phase which are very sensitive to the chemical composition of the nanograins. The amorphous ferromagnetic matrix basically provides the magnetic coupling between nanograins and the magnetoelastic energy balance. In the amorphous matrix, the saturation magnetization and magnetostriction constant are not altered significantly by small changes in its composition, contrary to what occurs in the crystalline phase [1]. Hence, for a proper soft magnetic design and for a better comprehension of the magnetic behavior of these materials, it is very important to determine the crystalline phase well, including its chemical composition.

$Fe_{73.5}Si_{13.5}B_9Nb_3Cu_1$ is a typical composition known as FINEMET™ and it is obtained from the devitrification of its precursor amorphous alloy by different heat, current or mechanical treatments. The process induces the nanocrystallization of the bcc-Fe phase with Si as solute element in solution. The solute content in the nanocrystals is unknown due to the fact that part of the Si remains in the amorphous matrix. Chemical composition of this phase, usually in the range of 15–25 at.% Si, can be determined by X-ray diffraction technique (XRD) via the lattice parameter measurements. When different species are present as solute elements in the bcc-Fe, XRD is insufficient to determine the chemical composition as the lattice parameter is affected in different ways for the solute species. Another common technique employed for structurally studying these systems, is the Mössbauer spectroscopy (MS) with ^{57}Co source, which gives us the information about the different environments of the Fe atoms either in nanocrystals or amorphous matrix, allowing the determination of some solute content in nanocrystals.

In the literature, there are several works which structurally studied, by XRD and MS techniques, FINEMET-like alloys with two different species of solute in the crystalline phase. Some of them provide the chemical composition of the nanograins using different approaches (sometimes not entirely clear). For example Borrego et al. [2] and Zorkovská et al. [3] in bcc Fe–Si–Al nanocrystals, Blázquez et al. in bcc Fe–Co–Ge nanocrystals [4], Gómez-Polo et al. [5], Borrego et al. [6] and Zbroszczyk et al. [7] in bcc Fe–Co–Si nanocrystals. In some other works, having the necessary data to determine the chemical composition, it is not reported due perhaps to the lack of a tool for this purpose (for example, [8] in bcc Fe–Si–Al and [9] in bcc Fe–Si–Ge nanocrystals). In previous works [10–12], we already employed these two techniques to approach the chemical composition of Fe–Si–Ge and Fe–Si–Al nanocrystals. In this work, we present some theoretical lattice parameter charts in the Fe-rich regions of the Fe–Si–Al, Fe–Si–Ge, Fe–Al–Ge, Fe–Co–Si, Fe–Co–Al, and Fe–Co–Ge ternary systems in order to validate the work previously performed by analyzing their structure based

* Corresponding author. Tel.: +54 387 4268539; fax: +54 387 4268502.
E-mail address: jmoya.fi.uba@gmail.com (J.A. Moya).

http://dx.doi.org/10.1016/j.jallcom.2015.01.014
0925-8388/

on phase diagrams and comparing the results obtained from these charts with experimental results in literature. We also extend the model for the mentioned systems and revise previous results in the perspective of the new data found in lattice parameters for the binary systems. The method and the charts provide a new tool for the determination of chemical composition in this kind of alloys in future works.

2. Material and methods

The method for the determination of the chemical composition of the crystalline phase in nanocrystalline alloys containing ternary nanocrystals consists in combining data of the lattice parameter of the nanocrystals obtained by XRD technique and its solute content data obtained by MS technique. The latter is calculated using binomial distributions [13] as it will be discussed in Section 2.2. Therefore, for combining these data, we also need to know the lattice parameters vs. chemical composition curves of the ternary alloys that are calculated here by means of a linear approach.

2.1. Calculus of the lattice parameter vs. chemical composition data in ternary alloys

For this purpose, we have developed some charts with the variation of the lattice parameter with composition in ternary systems under the assumption that there is a linear relationship between the lattice parameters of the binary alloys with the same solute content. For example, the lattice parameter of the $Fe_{80}Si_{15}Al_5$ ternary alloy will appear linearly interpolated between $Fe_{80}Si_{20}$ and $Fe_{80}Al_{20}$ binary alloys lattice parameters. It is known that a linear relationship in the lattice parameter with composition (under certain circumstances) was proposed in the Vegard's law [14]. However, deviations from this law sometimes appear and the linear assumption must be checked.

The charts containing the ternary phase lattice parameters were performed from the lattice parameter of the binary alloys shown in Fig. 1. These data were collected from literature and correspond to bcc-Fe solid solution with Si (a), Al (b), Ge (c) and Co (d). We also revised the phase structures on phase diagrams at room temperature and its types indicating their existence range along with the values of the lattice parameters in the same Fig. 1.

The Fe–Si system has a A2 structure type up to ~10 at.% Si. From then on, two kinds of ordered bcc structure types, B2 and $D0_3$, are present in the material up to ~26 at.% Si. Here, the B20 structure type appears together with the $D0_3$ [15]. The Fe–Al system also starts with the A2 structure in the Fe-rich region. Then, continues with (B2 + $D0_3$) and then with the $D0_3$ structure. In the range of 13–18 at.% some kind of ordering was also found [16]. According to the phase diagram, the phases in the Fe–Ge system from 0 to 20 at.% Ge are: A2 → B2 → (B2 + $D0_3$) → $D0_3$. From 20 at.% the $D0_3$ structure exists with the β phase, an hexagonal $B8_2$ structure [17]. Finally, the Fe–Co system forms a wide solid solution at room temperature up to 60 at.% Co with the A2 (less than ~10 at.% Co) and B2 structure types [18]. The A2 structure type corresponds to a bcc structure where the solute element can occupy any place in the cell; the B2 is an ordered bcc cell where the solute is placed in the center of the cube. The $D0_3$ superlattice consists of eight bcc cells formed by A2 and B2 structure types disposed alternatively in each direction. The lattice parameter of the $D0_3$ structure is then twice the one of the A2 or B2 structures types. So, for convenience, in all lattice parameter figures of this work, the ones of A2 and B2 are multiplied by two.

In the ternary phase diagrams of these systems, the presence of different phases or structures other than those above mentioned are not observed in the range of compositions of our interest [25–30]. The general behavior is the presence of the A2 structure in Fe-rich region (up to values close to 10% solute), then a small region with the B2 structure ending in the $D0_3$ or B2 + $D0_3$ structure types that extend approximately up to 25–35 at.% of solute content. When Al, Si or Co is added to the Fe–Ge alloy, the $D0_3$ structure predominates extending its existence range over the 25% and limiting the existence of the hexagonal β phase to a Fe–Ge rich region. In ternary diagrams with Co, the region of the B2 structure extends towards higher solute content. The lack of other structure than the bcc is important to make the linear approximation for the ternary phase lattice parameters.

2.2. Calculus of the solute content

Using Mössbauer spectroscopy on these materials (^{57}Co source), we can determined the content of Si, Al and/or Ge species in the bcc-Fe. These non-magnetic atoms modify the hyperfine parameters of the neighboring Fe atoms and, as a consequence, different subspectra can be identified on fitting the Mössbauer spectrum. From the relative fraction areas of these subspectra it is possible to determine the total content of Si, Al, or/and Ge in the bcc-Fe solid solution by means of the binomial distributions according to the structure types [13]. These atoms occupy the center of the cube in the B2 structure type and D sites in the $D0_3$ superlattice. In the case of Fe–Co alloys, the Co magnetic atom substitute the Fe in the B2 structure and occupy the sites A and C in the $D0_3$ structure [31]. They slightly modify the hyperfine parameters of the neighboring Fe and, consequently, no subspectra can be identified. Determination of chemical composition in Fe–Co binary alloy arises from small differences in the line broadening of the halfwidth of the outermost lines of spectrum [32] or in the hyperfine magnetic field value [33,34]. When a third atom species, as Si, Al or Ge, is added to the Fe–Co alloy, as well as when the Mössbauer spectrum has some amorphous components (like in nanocrystalline materials), the determination of the Co content through the hyperfine parameters is practically impossible. Therefore, in the case of Fe-based nanocrystals containing Co together with another solute, Mössbauer spectroscopy analysis can only determine the solute content of the species different from Co (i.e., the Si, the Al or the Ge content in the ternary alloys, in our case). In Fig. 2, we plot an example of Mössbauer spectrum and the fitted subspectra (S1–S6) for a $Fe_{73.5}Si_{11.5}Al_2Cu_1B_9Nb_3$ nanocrystallized alloy. In this case, the total solute content (nanocrystals) obtained in accordance with [13] was (Si + Al) = 19.8%.

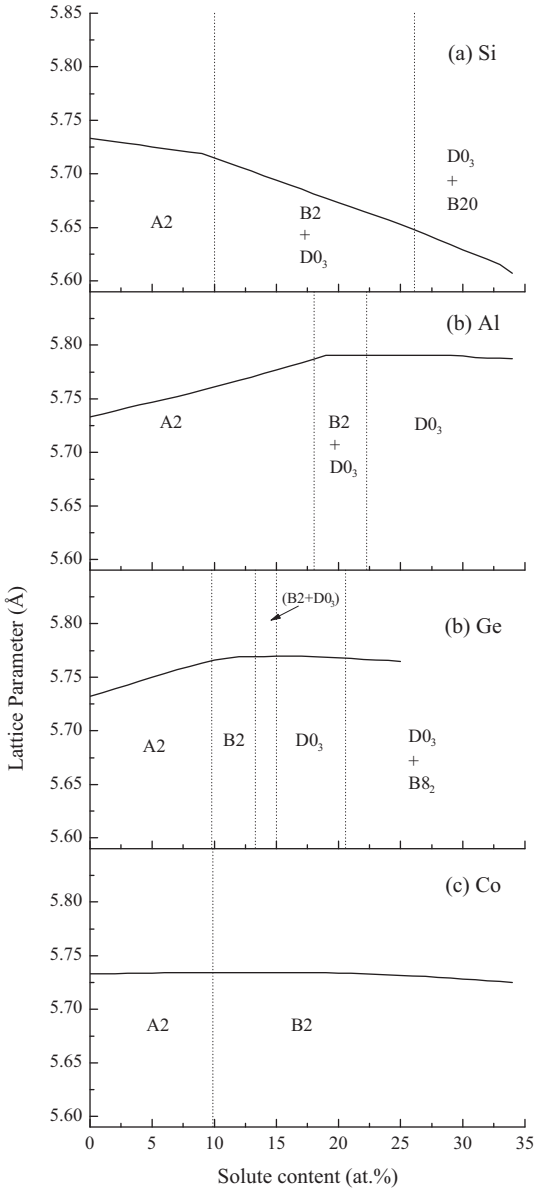

Fig. 1. Lattice parameters and structure types for bcc-Fe containing: (a) Si [19–21], (b) Al [19], (c) Ge [11,22,23] and (d) Co [21,24]. Al graphs are in the same scale for comparative purposes.

3. Calculation

From Figs. 3–8, we present the charts with the value of the lattice parameters of Fe-rich ternary solid solution for the Fe–Al–Si, Fe–Ge–Si, Fe–Al–Ge, Fe–Co–Si, Fe–Co–Al and Fe–Co–Ge systems, obtained from a linear relationship between the lattice parameter

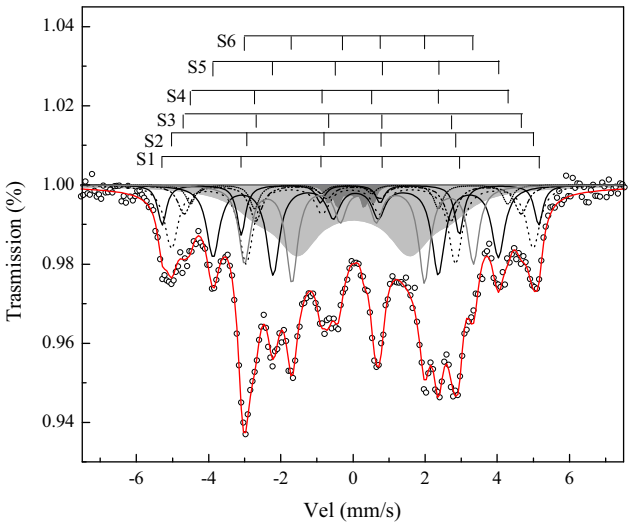

Fig. 2. Mössbauer spectrum and fit of nanocrystallized alloy $Fe_{73.5}Si_{11.5}Al_2Cu_1B_9Nb_3$.

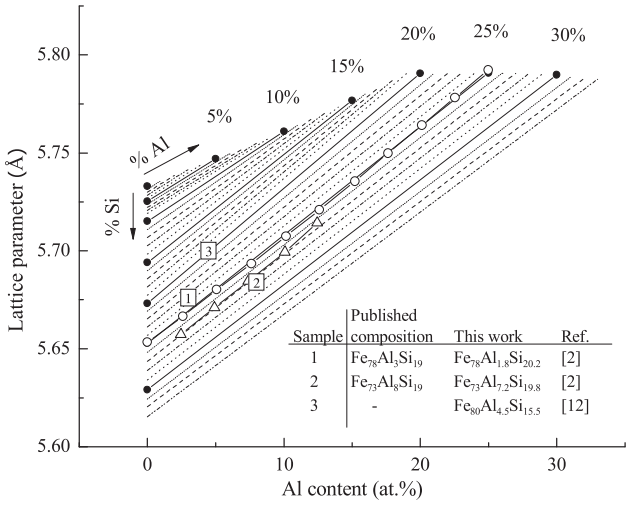

Fig. 3. Lattice parameter for the $Fe_{1-x}(Si,Al)_x$ system ($0 \leqslant x \leqslant 0.33$). Inset: table containing the published chemical composition data and the one obtained with this method. Sample numbers correspond to those in the numbered symbols.

data of the two binary alloys (from Fig. 1) with the same solute content. Each straight line in the charts represents a constant value of solute percentage as is indicated. The numbered symbols which appear in some of the charts correspond to the nanocrystallized alloys indicated in the respective inset tables. The open symbols represent the crystalline ternary alloys series employed for the chart validation (see Section 4). In systems without Co, one can obtain the chemical composition of the ternary phase by entering the straight line with the total solute content data obtained from MS (for example, 19.8% in the $Fe_{73.5}Si_{11.5}Al_2Cu_1B_9Nb_3$ nanocrystallized alloy mentioned above) and matching it with the lattice parameter data, a, obtained by XRD ($a = 5.70$ Å, in our example), or vice versa. In this way, we obtain the solute content in the alloy of the element indicated in the abscissa axis, (4.5% Al) and, by difference with the total content, the content of the second element. In the case of Co containing alloys, the procedure is similar, by entering in the chart with the solute content of the species diverse than Co (i.e., Si, Al, or Ge) which is the data obtained by MS. Interactive plots of these charts are available and accompany the electronic version.

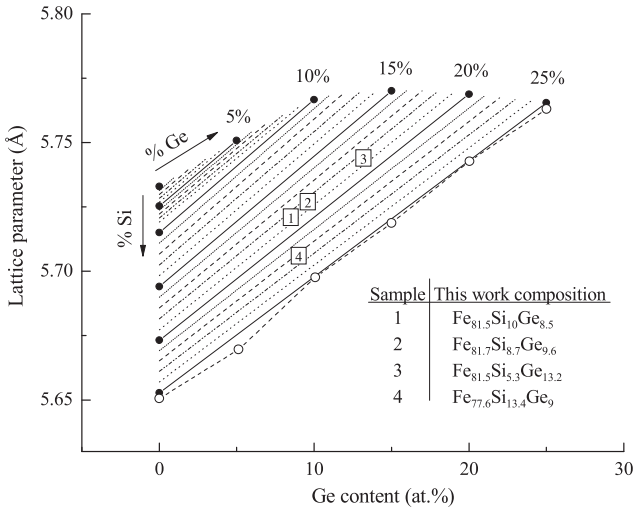

Fig. 4. Lattice parameter for the $Fe_{1-x}(Si,Ge)_x$ system ($0 \leqslant x \leqslant 0.25$). Inset: table with the chemical composition of our nanocrystals.

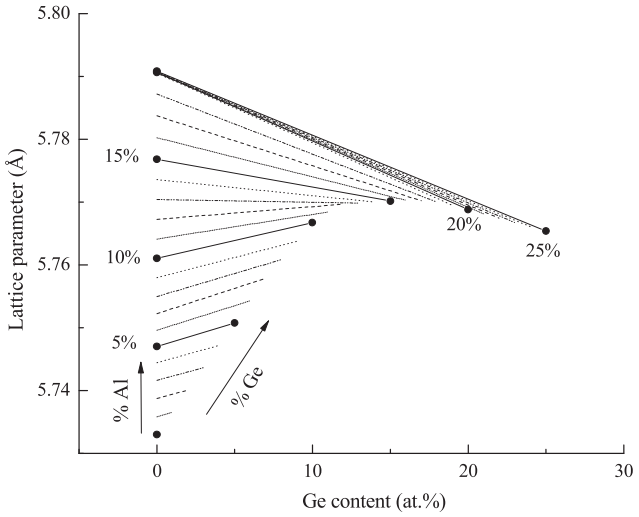

Fig. 5. Lattice parameter for the $Fe_{1-x}(Al,Ge)_x$ system ($0 \leqslant x \leqslant 0.25$).

In Fig. 4, we plot the results of chemical composition in some Fe–Ge–Si nanocrystals obtained previously by this method [10] (now revised, with more precise data on lattice parameters). With the available data of lattice parameters and solute compositions, we calculate the chemical composition of some ternary nanocrystals found in literature and are plotted in Figs. 3 and 6, comparing the chemical composition data reported and the one obtained by this method, as is shown in the inset tables.

4. Results and discussions

In order to validate the charts, we performed a thorough search of lattice parameters in ternary alloys for our six systems in the literature. These data are scarce, especially in the case of the Fe–Co–Ge system where no data was found. Either way, this chart is also presented and may serve for theoretical approaches and for a future verification.

In the Fe–Si–Al system, Cowdery [35] found a near parabolic relationship between the experimental lattice parameter of $Fe_{75}Si_{25}$ and $Fe_{75}Al_{25}$. These results are also shown in Fig. 3 in a very good accordance with our linear approach: the greatest difference

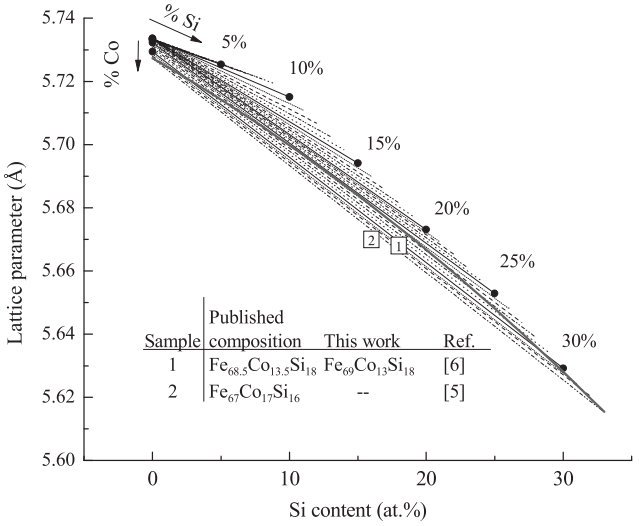

Fig. 6. Lattice parameter for the $Fe_{1-x}(Co,Si)x$ system ($0 \leqslant x \leqslant 0.33$). The thick gray curve corresponds to a proposed parabolic relationship between the $Fe_{67}Co_{33}$ and $Fe_{67}Si_{33}$ lattice parameter values (see Section 4).

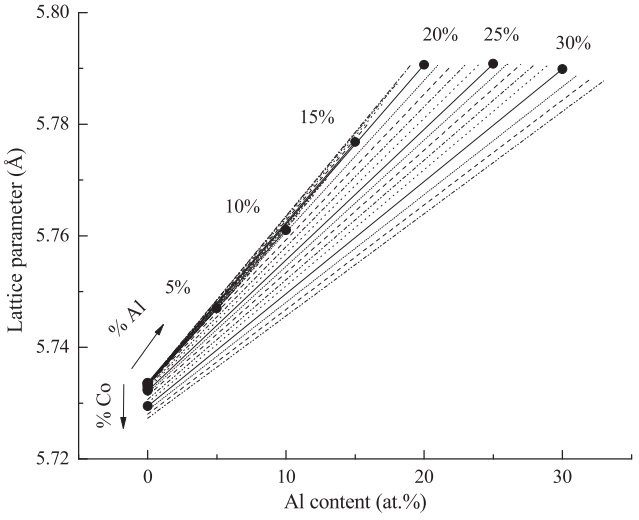

Fig. 7. Lattice parameter for the $Fe_{1-x}(Co,Al)_x$ system ($0 \leqslant x \leqslant 0.33$).

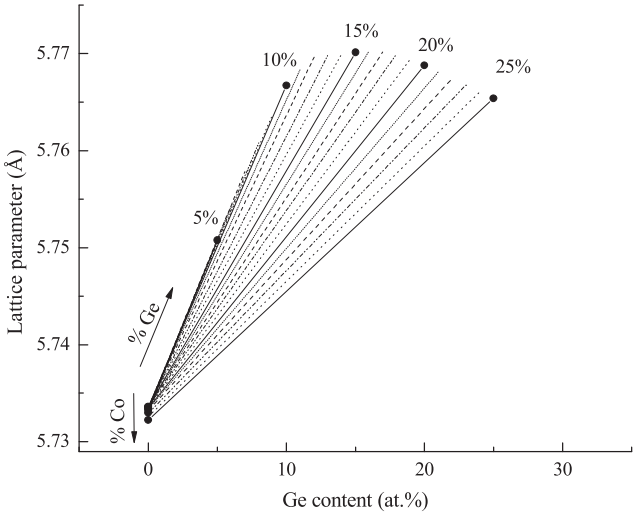

Fig. 8. Lattice parameter for the $Fe_{1-x}(Co,Ge)_x$ system ($0 \leqslant x \leqslant 0.25$).

between these curves is less than 1% of the total solute content. In the same Fig. 3, it is shown the lattice parameters of some alloys in the series $Fe_{73}(Si_{1-x}Al_1)_{27}$ with analogous results.

In the Fe–Si–Ge system (Fig. 4), Arzhnikov [36] found also an approximate linear relationship between the lattice parameter of $Fe_{75}Si_{25}$ and $Fe_{75}Ge_{25}$ in accord with our interpolation.

In Fig. 9, we show some experimental results of lattice parameters obtained from literature for the series $Fe_{75-x}Co_xAl_{25}$ and $Fe_{75-x}Co_xSi_{25}$ and the ones obtained from our approximation. In the case of Fe–Co–Al system, our approach is in good accordance with the results of [34], within the limits of the experimental error bars, and decreasing with the same slope. With respect to the Fe–Co–Si system, our approach differs significantly from the experimental results obtained by [31,37]. The initial value for the binary alloy $Fe_{75}Co_{25}$ is average between both experimental ones, but with the replacement of Fe with Co, our calculated lattice parameters decrease more rapidly than those from experimental results. This deviation can be explained by the correlation between magnetic moments and interatomic distances in alloys including 3d transition metals as proposed in [31,38]. In our opinion, a parabolic relationship instead of a linear one must be considered (similar to the case of the Fe–Si–Al system). One example of parabolic relationship was performed in Fig. 6 between the lattice parameter values of the alloys $Fe_{67}Co_{33}$ and $Fe_{67}Si_{33}$ using an average experimental data for the alloy $Fe_{67}Co_8Si_{25}$ obtained from [31,38]. According to these results, the published values for the nanocrystals compositions $Fe_{67}Co_{17}Si_{16}$ [5] and $Fe_{68.5}Co_{13.5}Si_{18}$ [6] obtained with different approaches (probably linear ones), with $a = 5.670$ Å and 5.668 Å respectively, will need a Si content of about 20% to remain within the chart performed with parabolic relationships. These aspects will be addressed in a future work.

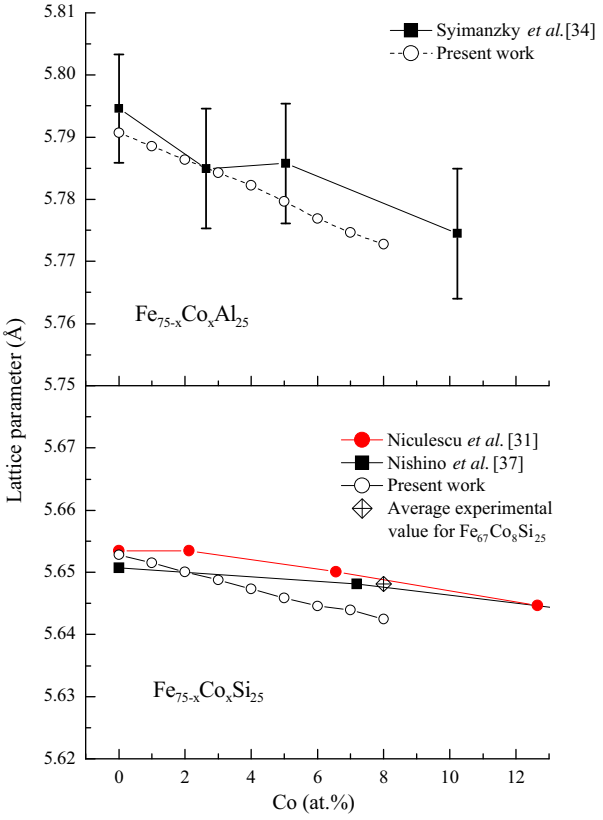

Fig. 9. Experimental values (filled symbols) and theoretical approach (open symbols) for the lattice parameter in the series $Fe_{75-x}Co_xAl_{25}$ (a) and $Fe_{75-x}Co_xSi_{25}$ (b). Both graphs have the same increment in scales for comparative purposes.

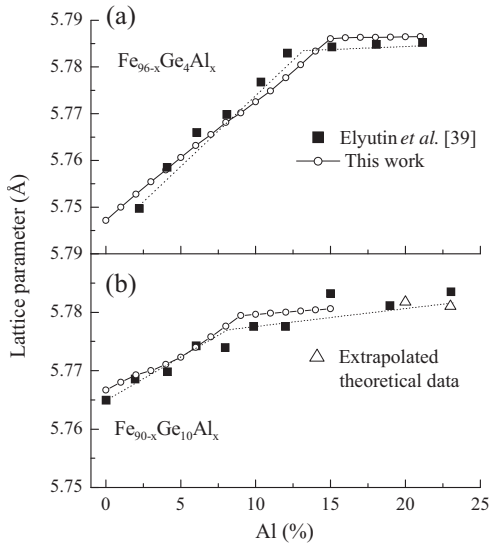

Fig. 10. Experimental values (solid symbols), theoretical approach (open symbol, ○) and theoretical extrapolated data (open symbol, △) for the lattice parameters in the series $Fe_{96-x}Ge_4Al_x$ and $Fe_{90-x}Ge_{10}Al_x$. The dotted lines are the eye guide of Ref. [39].

Experimental lattice parameters on the series $Fe_{96-x}Ge_4Al_x$ and $Fe_{90-x}Ge_{10}Al_x$ [39] are compared with the ones obtained with the linear approach for the system Fe–Ge–Al in Fig. 10, and they show a very good agreement. In the case of the series $Fe_{90-x}Ge_{10}Al_x$ we can complete up to 25% of solute content due to the uncertainties in the lattice parameter that the Fe–Ge binary system due to the presence of the β phase with the orthorhombic structure. However, the addition of Al stabilizes the $D0_3$ phase in this ternary system. Interestingly, if we assume that the lattice parameter of $Fe_{75}Ge_{25}$ = $Fe_{70}Ge_{30}$ = $Fe_{65}Ge_{35}$ we can extrapolate the last two points of this series that also fit the experimental ones.

5. Conclusions

Theoretical values of lattice parameters were determined for the bcc $Fe_{1-x}(M,N)_x$ ternary systems with M and N = Si, Al, Ge or Co, and $0 \leqslant x \leqslant \sim 0.3$. Charts containing these values were validated with experimental data finding a good correspondence between the experimental and the determined values. One exception was found in the Fe–Co–Si system where significant difference in terms of chemical composition was found, although the deviation is small in terms of lattice constant. Therefore, we propose to review this system in a future work by applying a parabolic relationship. Since it was found that the linear approximations of the lattice parameters made in this work do not always fit the experimental ones, the Fe–Co–Ge system still needs a validation as no experimental data was found for this work.

Using these charts and the data provided by XRD and MS techniques we were able to satisfactorily determine the chemical composition in some ternary Fe-based nanocrystals from nanocomposite alloys.

These charts can be employed to check the chemical compositions of ternary alloys and also for some theoretical calculus without the need of producing the alloy.

Appendix A. Supplementary material

Supplementary data associated with this article can be found, in the online version, at http://dx.doi.org/10.1016/j.jallcom.2015.01.014.

References

[1] J.A. Moya, Improving soft magnetic properties in FINEMET-like alloys. A study, J. Alloys Comp. 622 (2015) 635–639, http://dx.doi.org/10.1016/j.jallcom.2014.10.124.
[2] J.M. Borrego, A. Conde, I. Todd, M. Frost, H.A. Davies, M.R.J. Gibbs, et al., Nanocrystallite compositions for Al- and Mo-containing finemet-type alloys, J. Non-Cryst. Solids 287 (2001) 125–129, http://dx.doi.org/10.1016/S0022-3093(01)00546-4.
[3] A. Zorkovská, J. Kováč, P. Sovák, P. Petrovič, M. Konč, Structure and magnetic behaviour of Fe–Cu–Nb–Si–B–Al alloys, J. Magn. Magn. Mater. 215–216 (2000) 492–494, http://dx.doi.org/10.1016/S0304-8853(00)00201-8.
[4] J.S. Blázquez, V. Franco, A. Conde, Mössbauer study of a Fe–Zr–B–Cu–(Ge, Co) nanocrystalline alloy series, J. Alloys Comp. 422 (2006) 32–39, http://dx.doi.org/10.1016/j.jallcom.2005.12.004.
[5] C. Gómez-Polo, P. Marín, L. Pascual, A. Hernando, M. Vázquez, Structural and magnetic properties of nanocrystalline $Fe_{73.5-x}Co_xSi1_{3.5}B_9CuNb_3$ alloys, Phys. Rev. B 65 (2001), http://dx.doi.org/10.1103/PhysRevB.65.024433.
[6] J.M. Borrego, C.F. Conde, A. Conde, J.M. Greneche, Microstructural properties of (Fe, Co)SiBCuNb nanocrystalline alloys, J. Phys. Condens. Matter. 14 (2002) 883–893, http://dx.doi.org/10.1088/0953-8984/14/4/321.
[7] J. Zbroszczyk, K. Narita, J. Olszewski, W. Ciurzyńska, W. Lijun, B. Wysłocki, et al., Effect of Co addition on the microstructure and magnetic properties of Fe–Cu–Nb–Si–B alloy, J. Magn. Magn. Mater. 160 (1996) 281–283, http://dx.doi.org/10.1016/0304-8853(96)00199-0.
[8] D. Prabhu, A. Narayanasamy, K. Ganesan, N. Ponpandian, K. Chattopadhyay, Exchange field penetration in $Fe_{73.5}Cu_1Mo_3Si_{12.5}Al_1B_9$ alloy, J. Alloys Comp. 438 (2007) 15–20, http://dx.doi.org/10.1016/j.jallcom.2006.08.011.
[9] A. Puszkarz, M. Wasiak, P. Uznański, P. Sovak, M. Moneta, Structural properties and Mössbauer spectroscopy of finemet™ doped with Ge, Vacuum 83 (2009) S245–S248, http://dx.doi.org/10.1016/j.vacuum.2009.01.073.
[10] J.A. Moya, V.J. Cremaschi, H. Sirkin, From Fe_3Si towards Fe_3Ge in finemet-like nanocrystalline alloys: Mössbauer spectroscopy, Phys. B Condens. Matter. 389 (2007) 159–162, http://dx.doi.org/10.1016/j.physb.2006.07.046.
[11] J.A. Moya, Nanocrystals and amorphous matrix phase studies of finemet-like alloys containing Ge, J. Magn. Magn. Mater. 322 (2010) 1784–1792, http://dx.doi.org/10.1016/j.jmmm.2009.12.030.
[12] J.A. Moya, S. Gamarra Caramella, L.J. Marta, C. Berejnoi, Design parameters for nanostructured soft magnetic alloys, IEEE Trans. Magn. 49 (2013) 4664–4667, http://dx.doi.org/10.1109/TMAG.2013.2259149.
[13] G. Rixecker, P. Schaaf, U. Gonser, On the interpretation of the Mössbauer spectra of ordered Fe–Si alloys, Phys. Status Solidi A 139 (1993) 309–320, http://dx.doi.org/10.1002/pssa.2211390205.
[14] L. Vegard, Die Konstitution der Mischkristalle und die Raumfullung der Atome, Z. Phys. 5 (1921) 17–26, http://dx.doi.org/10.1007/BF01349680.
[15] O.K. von Goldbeck, Fe—Si Iron—Silicon, in: IRON—Binary Phase Diagr., Springer Berlin Heidelberg, Berlin, Heidelberg, 1982, pp. 136–139, http://dx.doi.org/10.1007/978-3-662-08024-5_62.
[16] B. Predel, Al–Fe (aluminum-iron), in: O. Madelung (Ed.), Ac–Au – Au–Zr, Springer-Verlag, Berlin/Heidelberg, 1991, pp. 1–10, http://dx.doi.org/10.1007/10000866_104.
[17] B. Predel, Fe–Ge (iron–germanium), in: O. Madelung (Ed.), Dy–Er – Fr–Mo, Springer-Verlag, Berlin/Heidelberg, 1995, pp. 1–5, http://dx.doi.org/10.1007/10474837_1302.
[18] H. Okamoto, Co–Fe (cobalt–iron), J. Phase Equilib. Diffus. 29 (2008) 383–384, http://dx.doi.org/10.1007/s11669-008-9345-5.
[19] R.M. Bozorth, Ferromagnetism, IEEE Press, Piscataway, N.J., 1961.
[20] B. Predel, Fe–Si (iron–silicon), in: O. Madelung (Ed.), Dy–Er – Fr–Mo, Springer-Verlag, Berlin/Heidelberg, 1995, pp. 1–6, http://dx.doi.org/10.1007/10474837_1340.
[21] W.B. Pearson, G.V. Raynor, A handbook of lattice spacings and structures of metals and alloys, 1964, ISBN: 9781483213187.
[22] H. Chessin, S. Arajs, R.V. Colvin, D.S. Miller, Paramagnetism and lattice parameters of iron-rich iron–germanium alloys, J. Phys. Chem. Solids 24 (1963) 261–273, http://dx.doi.org/10.1016/0022-3697(63)90131-8.
[23] E.V. Voronina, G.N. Konygin, A.N. Deyev, V.V. Kriventsov, E.P. Yelsukov, EXAFS investigation of the local atomic structure of Fe–Ge nanocrystalline disordered alloys, Crystallogr. Rep. 51 (2006) S183–S191, http://dx.doi.org/10.1134/S1063774506070261.
[24] B. Predel, Co–Fe (cobalt–iron), in: O. Madelung (Ed.), Ca–Cd – Co–Zr, Springer-Verlag, Berlin/Heidelberg, 1993, pp. 1–13, http://dx.doi.org/10.1007/10086082_911.
[25] V. Raghavan, Al–Fe–Si (aluminum–iron–silicon), J. Phase Equilibria. 23 (2002) 362–366, http://dx.doi.org/10.1361/105497102770331604.
[26] V. Raghavan, Fe–Ge–Si (iron–germanium–silicon), J. Phase Equilibria. 23 (2002) 443–444, http://dx.doi.org/10.1361/105497102770331433.
[27] V. Raghavan, Al–Fe–Ge (aluminum–iron–germanium), J. Phase Equilibria. 23 (2002) 437–438, http://dx.doi.org/10.1361/105497102770331398.
[28] V. Raghavan, Co–Fe–Si (cobalt–iron–silicon), J. Phase Equilibria. 15 (1994) 527–528, http://dx.doi.org/10.1007/BF02649407.
[29] V. Raghavan, Al–Co–Fe (aluminum–cobalt–iron), J. Phase Equilibria. 15 (1994) 408, http://dx.doi.org/10.1007/BF02647562.
[30] V. Raghavan, Co–Fe–Ge (cobalt–iron–germanium), J. Phase Equilibria. 23 (2002) 411, http://dx.doi.org/10.1361/105497102770331415.

[31] V. Niculescu, J. Budnick, W. Hines, K. Raj, S. Pickart, S. Skalski, Relating structural, magnetic-moment, and hyperfine-field behavior to a local-environment model in $Fe_{3-x}Co_xSi$, Phys. Rev. B 19 (1979) 452–464, http://dx.doi.org/10.1103/PhysRevB.19.452.
[32] T. Kamimori, M. Shida, M. Goto, H. Fujiwara, Investigation of ordering in $Fe_{3-x}Co_xSi$ by Mössbauer spectroscopy and magnetocrystalline anisotropy, J. Magn. Magn. Mater. 54–57 (1986) 927–928, http://dx.doi.org/10.1016/0304-8853(86)90317-3.
[33] C. Johnson, M. Ridout, T. Cranshaw, P. Madsen, Hyperfine field and atomic moment of iron in ferromagnetic alloys, Phys. Rev. Lett. 6 (1961) 450–451, http://dx.doi.org/10.1103/PhysRevLett. 6.450.
[34] K. Szymański, M. Biernacka, L. Dobrzyński, K. Perzyńska, K. Rećko, D. Satuła, et al., Mössbauer and magnetic studies of $Fe_{3-x}Co_xAl$, J. Magn. Magn. Mater. 210 (2000) 150–162, http://dx.doi.org/10.1016/S0304-8853(99)00644-7.
[35] S.J. Cowdery, Lattice parameters of iron–aluminum silicon alloys with the DO/sub 3/structure, Ames Lab., IA (USA), US, 1979. doi: 6517800-phvyS5.
[36] A.K. Arzhnikov, Magnetic moments and hyperfine magnetic fields in ordered and disordered quasi-binary Fe75 (Si 1–xGe x)25 Alloys, Phys. Solid State 47 (2005) 2063, http://dx.doi.org/10.1134/1.2131146.
[37] Y. Nishino, S. Inoue, S. Asano, N. Kawamiya, Anomalous temperature dependence of the electrical resistivity in binary and pseudobinary alloys based on Fe_3Si, Phys. Rev. B 48 (1993) 13607–13613, http://dx.doi.org/10.1103/PhysRevB.48.13607.
[38] M. Shiga, Correlation Between Lattice Constant and Magnetic Moment in 3d Transition Metal Alloys, in: ASCE, 1974: pp. 463–477. doi:10.1063/1.3141758.
[39] O.P. Elyutin, M.K. Khachatryan, Structure and properties of Fe–Al–Ge alloys, Met. Sci. Heat Treat. 14 (1972) 946–949, http://dx.doi.org/10.1007/BF00651984.